ONECENTRAL PRESS

Available online at www.onecentralpress.com

One Central Press

journal homepage: www.onecentralpress.com/functional-nanostructures

Microwave Synthesis of Aluminium Doped ZnO Nanostructures and Characterization

D. Selvakumari[1,2a], C.S. Abraham[1,b], P. Subhashini[1,c], N. Lakshminarayan[1,d]*

[1] *Madras Christian College, East Tambaram, Chennai 600059, India.*
[2] *currently @ Elmhurst College, 190 Prospect Ave, Elmhurst, Illinois 60126, USA.*
[*] *Corresponding author*

ABSTRACT

Nanocrystalline Al doped ZnO (AZO) nanostructures have been synthesized by a simple surfactant free thermal decomposition method in a microwave oven. Zinc nitrate hexa hydrate and ethylene glycol were used as the precursor materials to prepare ZnO and aluminum nitrate was added for Aluminium doping (1 to 7%). The samples were characterized by X-ray diffraction (XRD), Transmission electron microscopy (TEM), UV- visible spectroscopy (UV), Photoluminescence (PL), Energy Dispersive X-Ray Spectroscopy (EDX) and Impedance Spectroscopy (IS). Analyses show that the Al doping significantly affected the crystalline nature, particle size, optical properties and conductivity of the processed ZnO nanoparticles. The XRD spectra indicate that the ZnO crystal has a hexagonal wurtzite structure. TEM images show the lattice arrangement of atoms in hexagonal shapes. The optical properties of the samples are investigated by measuring the UV-VIS absorption at room temperature. There was a variation in particle size in the range of 20nm to 52nm, with incorporation of dopant. Also, the band gap seemed to be influenced by dopant concentration, with a high value of 3.202eV for 5% doping. A tenfold increase of conductivity (0.302 to 3.75 (m Ω cm) $^{-1}$) results with Al doping.

I. INTRODUCTION

Zinc oxide (ZnO) in its nanostructures has been attracting a lot of attention both for fundamental studies and different applications from sensors to optoelectronic devices. It is a II–VI group compound semiconductor which crystallizes in wurtzite structure [1, 2] with a wide band gap of 3.4 eV and a large exciton binding energy at room temperature. ZnO has characteristics of high transparency in visible range, good UV trapping properties, non-toxicity, natural abundance etc., These unique properties enable potential applications such as catalysts, drug carriers, sensors, pigments, magnetic, optical materials and also in biological applications [3] and cancer diagnosis and treatments [4] etc. The electrical resistivity of the ZnO in the order of 0.75 MΩ at room temperature can be further reduced by doping with group III elements. AZO is receiving greater attention as being a valuable alternative to ITO due to its increased optical transmittance in the visible range and low electrical resistivity [5, 6, 7, 8]. A variety of nanostructures of ZnO like spheres, rods, disks, rings, ribbons, nails and flowers have been synthesized by various physical and chemical methods. [8, 9, 10] The most commonly adopted methods like mechano chemical methods, precipitation, sol- gel method, hydrothermal processes, combustion methods, sono-chemical etc., would involve sophisticated equipment, high temperatures and time consuming tedious methods for large scale production. Microwave syntheses [11, 12, 13] are attracting researches owing to unique features like simpler apparatus, highly localized heating and hence energy efficient with faster process time. Consequently, scaling becomes easier.

In this paper we report the synthesis of hexagonal shaped un-doped ZnO Nano disks and Aluminium doped ZnO nanostructures using microwave heating. Due to the specific rapid agitation of only the reactants in the mixture, by the microwave energy, the reaction process is better enabled (around 15 minutes) and energy efficient. Highly crystalline ZnO nanostructures have been synthesized in a very short time. The synthesis was carried out with optimal power and on/off radiation cycles, for they may have a great effect on the structure and properties of the products, as reported earlier [11, 12, 13]. The synthesized product

was characterized by XRD, TEM, UV-Vis and impedance spectroscopy measurements. This simple, quick, cost effective and energy saving method could be scaled up easily for the production of highly pure and crystalline un-doped and Al doped ZnO nanostructures.

II. EXPERIMENT

Powder Preparation. The AZO Nano powders were synthesized from $Zn(NO_3)_2$ $6H_2O$, $Al(NO_3)_3$ $9H_2O$ and Ethylene Glycol. All of the reagents involved in the experiments were of analytical grade, Merck make and utilized as received without further purification. The synthesis was carried out in a domestic microwave oven (Samsung Microwave oven [MD 73AD] with a power source of 230V – 50 Hz.

For forming ZnO powder, 5.503 g of zinc nitrate hexa hydrate was mixed with 3-5 drops of ethylene glycol and stirred well till a homogenous paste like substance was attained. The contents were transferred to a microwave safe container. The dish was then placed in a microwave and heated with a power of 300W. On heating thermal decomposition takes place to form zinc oxide.

$$2\ Zn(NO_3)_2 \rightarrow 2\ ZnO + 4\ NO_2 + O_2$$

The reactants were heated for 10 minutes with on/off cycles of 30/10 sec. The contents in the dish were then transferred to a culture tube after cooling down to room temperature.

To prepare 1 to 7% atomic weight percentage AZO nanostructures, appropriate measures of aluminum nitrate were added to zinc nitrate and 2-3 drops of ethylene glycol reaction mixture and stirred well till a homogenous solution was attained. The above heating procedure was repeated and the resultant powders were investigated with XRD, TEM, PL, UV-Visible and Impedance Spectroscopy techniques.

The crystalline structure of the nanostructures was determined by SEIFERT JSO DEBYEFLEX 2002 (Germany make) X-ray diffractometer equipment, using the CuK® line (1.5406 A°) with an accelerating voltage of 40KV. The un-doped and 7% Aluminium doped ZnO samples topography, morphology and elemental composition were by transmission electron microscope (model JEM 2100/ JEOL/ 200KV /LaB6 filament). The optical absorption and transmission spectra were measured using UV-VIS-NIR spectrometer (Cary 5E) within 280–900 nm. The Impedance Spectroscopy studies were conducted on pressed disc shaped samples (8mm diameter) using Solartron SI1260 Impedance Gain-phase analyzer. The Photoluminescence studies of the sample were carried out using the Jobin Yvon Flourolog-3-11 spectro-fluorometer in the 250-800 nm range.

III. RESULTS AND DISCUSSION

Structures and Composition of AZO Nano powders. Fig 1 shows the XRD pattern of un-doped and 1 to 7% Al doped ZnO samples. The diffraction planes (100), (002), (101), (102), (110), (103), (200), (112), and (201) in the patterns can be perfectly indexed to the hexagonal wurtzite phase structure (JCPDS PDF Card-36-1451). Also no diffraction peaks corresponding to Zn, $Zn(OH)_2$, Al_2O_3 and other impurities are observed. No aluminum phase detection in the XRD patterns may be due to substitution of Al ions in the Zn sites entirely in the lattices of ZnO crystal [14]. The values of lattice spacing as calculated by the XRD data are in good agreement with those obtained from TEM analysis. Zinc oxide crystallizes in three forms: hexagonal wurtzite, cubic zinc blende, and the rarely observed cubic rock salt. The wurtzite structure is most stable and thus most common at ambient conditions [1]. The highly localized specificity of the energy supply to the reactants and instantaneous reversion to ambient conditions seem to enable the formation of the most stable structure, in this fast process with low thermal budgeting. XRD analysis indicates that the pure ZnO phase is obtained in all the samples. The average particle sizes of the un-doped and 0- 7 % Al doped ZnO samples were calculated using the Debys Scherrer Formula for (002) planes.

Table 1 Particle Size and d spacing values calculated for different Al dopants of ZnO Nano powders.

SAMPLE	Average Particle Size [nm]	d [A°]
ZnO	20.629	2.45
AZO 1%	40.07	2.46
AZO 2%	52.25	2.47
AZO 3%	42.76	2.47
AZO 4%	47.26	2.47
AZO 5%	42.71	2.47
AZO 6%	40.99	2.45
AZO 7%	46.24	2.476

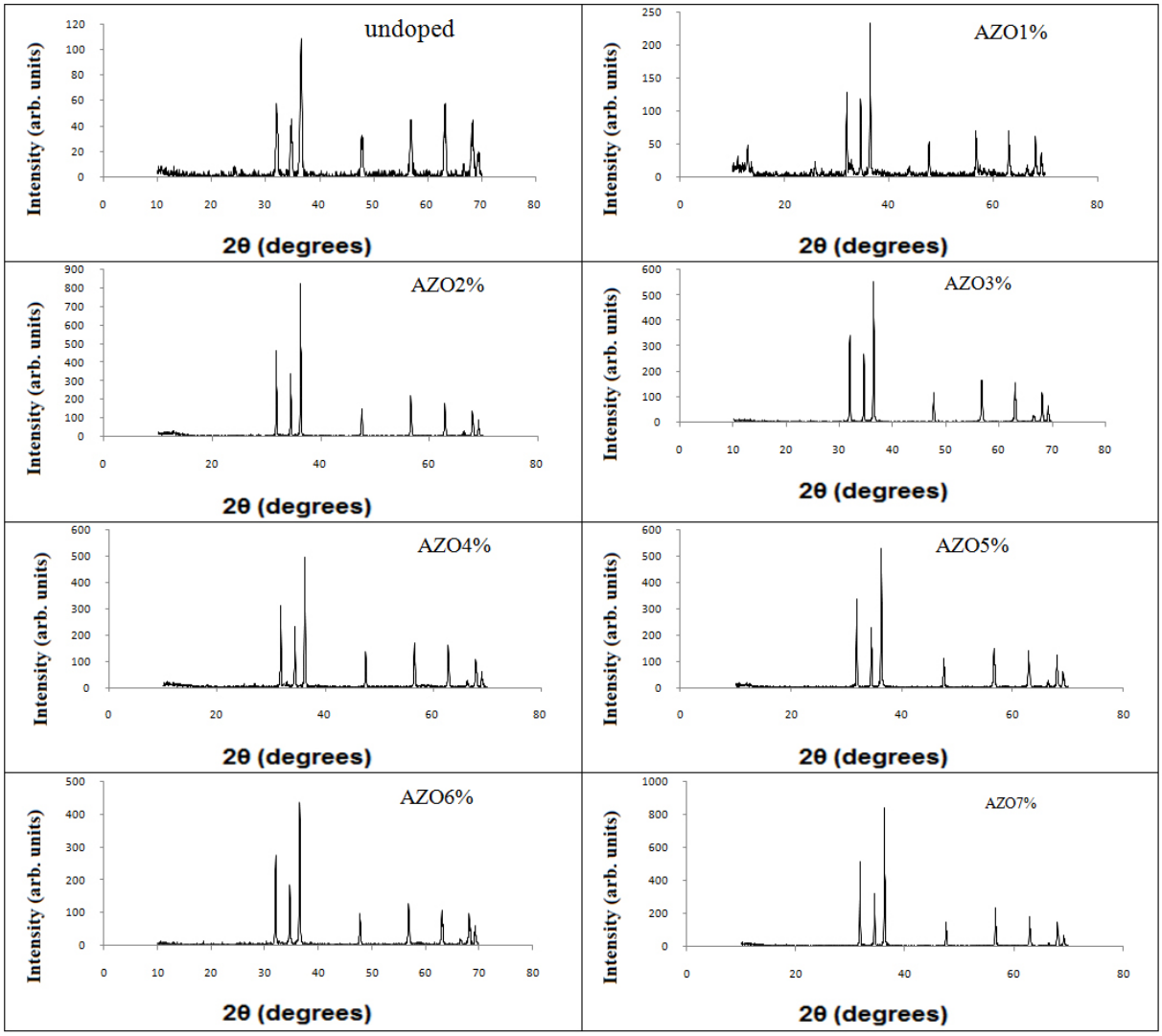

Figure 1 XRD scans for different Al dopant concentrations of ZnO Nano powders.

Structure analysis. Morphology of un-doped and 7% Al-doped ZnO nanoparticles was investigated by FETEM. Fig. 2 represents the micrographs of un-doped and Al-doped ZnO nanoparticles, respectively. These images demonstrated that grown nanoparticles were uniform sized and hexagonal shaped with particle size in the order of ~ 40 nm. High resolution TEM images show that particles were crystalline and conform with XRD data. TEM Micrographs clearly show the typical hexagonal lattice structure of as prepared un-doped ZnO Nanoparticles. The TEM image of the 7% Al doped ZnO sample with high magnification displays ordered hexagonal-like spot arrays, which confirms the formation of the hexagonally arranged lattice. The lattice spacing 'd' from the TEM images were also found to be in good agreement with that obtained from the XRD analysis. TEM Micrographs clearly indicate un-doped ZnO Nanoparticles having definite boundaries between hexagonal crystals and Aluminium doped ZnO Nano powders show merged boundaries between crystals. 7 % Al-doped ZnO Nano powders show substantially deteriorated in-plane ordering. This may be owing to smaller ionic radius Al atoms replacing the Zn atoms with relatively bigger ionic radius.

Optical properties. Optical absorption spectra of un-doped and 0-7 at % AZO Nano powders were recorded in the wavelength region of 250–800 nm. Fig. 3 shows the plots of transmission versus wavelength and the inset shows the plots of first derivative of absorption against photon energy. The presence of a single predominant peak in the plots suggests that the nanostructures have direct and allowed transition. It is also well known that ZnO is a direct band-gap material [1] and the energy gap (E_g) can thus be estimated by assuming direct transition between conduction band and valence bands. The energy corresponding to the maximum peak points in the dA/dE vs Energy graph [fig. 4], gives band gap energy of the Al-doped ZnO Nano powders [15]. The optical band gap varies between 3.161 to 3.202 eV (Fig 3). Such unusual red-shift of fundamental absorption edge has been reported by Vijay Kumar et al., [14] and has been explained in terms of stress relaxation mechanism. Similar results observed in our present work may be due to the introduction of defect states within the band gap. Formation of such impurity levels gives rise to new donor electronic states just below the conduction band. This arises due to hybridization between states of the ZnO matrix and of the Al dopant.

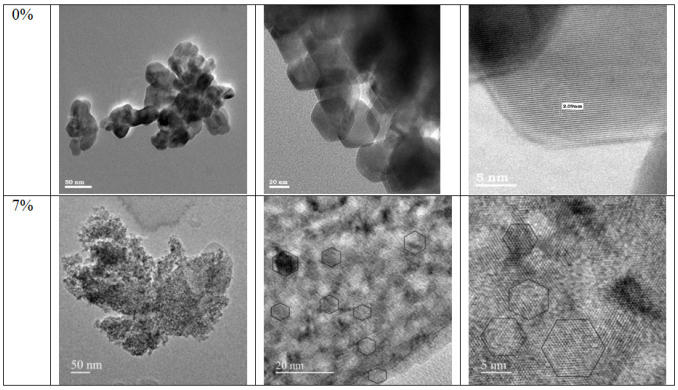

Figure 2 TEM Micrographs of undoped ZnO and 7% Al doped ZnO nanopowder samples.

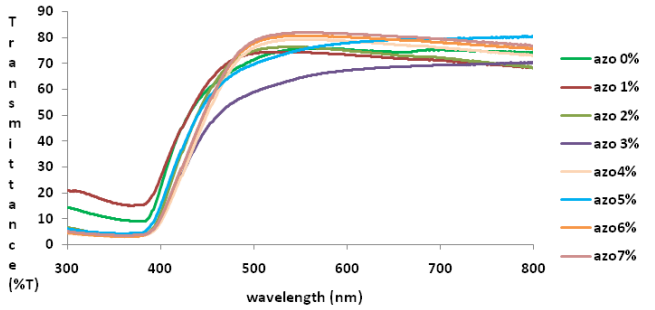

Figure 3 Optical Transmission spectra of 0-7 at % AZO Nano powders.

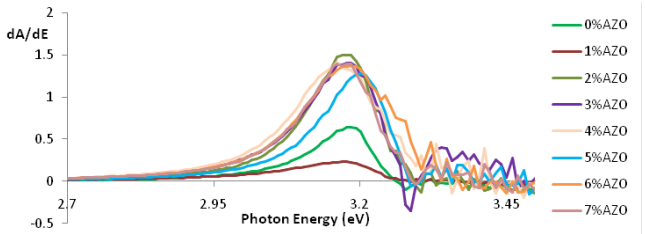

Figure 4 dA/dE vs Energy graph of 0-7 at % AZO Nano powders.

Table. 2 shows the variation of band gap with Al doping percentage. The Band gap increases considerably up to 5% of Al doping and decreases with further increase in doping %. According to normal doping rules, substitution of Al3+ at the Zn2+ sites creates one extra free carrier in the process and occupies Zn2+ sites up to the solubility. Therefore, increase of carrier concentration up to the solubility limit is logical but beyond solubility limit a new phase of Al_2O_3 arises and therefore substitution of Al is no longer effective as before. As a result, concentration of carriers starts to decrease above 5% of Al, in accordance with earlier reports where this effect on the optical bandgap is associated with the increase of crystallites size [16].

Table 2 Variation of band gap with Al doping percentage.

Al doping %	Bandgap (eV)
ZnO	20.629
AZO 1%	40.07
AZO 2%	52.25
AZO 3%	42.76
AZO 4%	47.26
AZO 5%	42.71
AZO 6%	40.99
AZO 7%	46.24

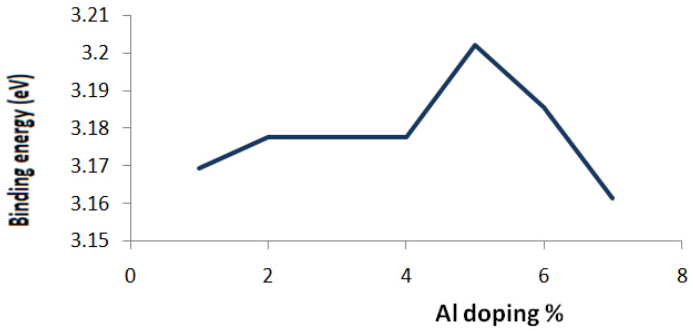

Photoluminescence measurements. Figure 5 shows the room-temperature PLE spectra of the undoped and 1-7% Al doped ZnO samples as a function of the photon energy. The PLE spectra of all the samples exhibited a characteristic near-band-edge (NBE) at about 3.48 eV (UV region) and a deep-level emission centered at around 2.66 eV (blue-green region). The NBE intensity tended to decrease markedly with Al addition in the samples. The NBE emission is known to result from the direct recombination of electron hole pairs. Thus, the energy of the NBE emission is a direct measure of the band gap. Generally, luminescence properties of the nanomaterials have a close relation with crystallinity because the density of defects reduces with an improvement of the crystallinity. The NBE and other features of the PLE and their respective variations with doping are indicative of the defect structure consequent to in-plane disordering [17]. The deep-level emission (blue-green region) originates from point defects, such as oxygen vacancies and interstitial Zn2+ sites [17,18].

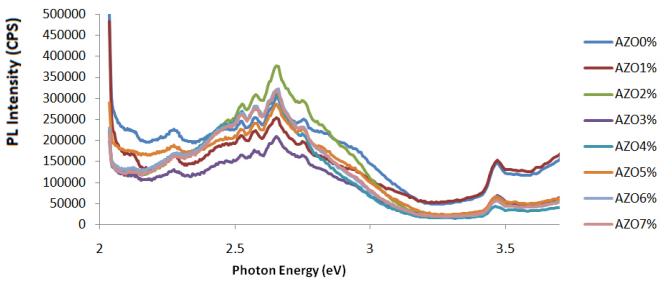

Figure 5 PLE spectra of the undoped and 1-7% Al doped ZnO samples.

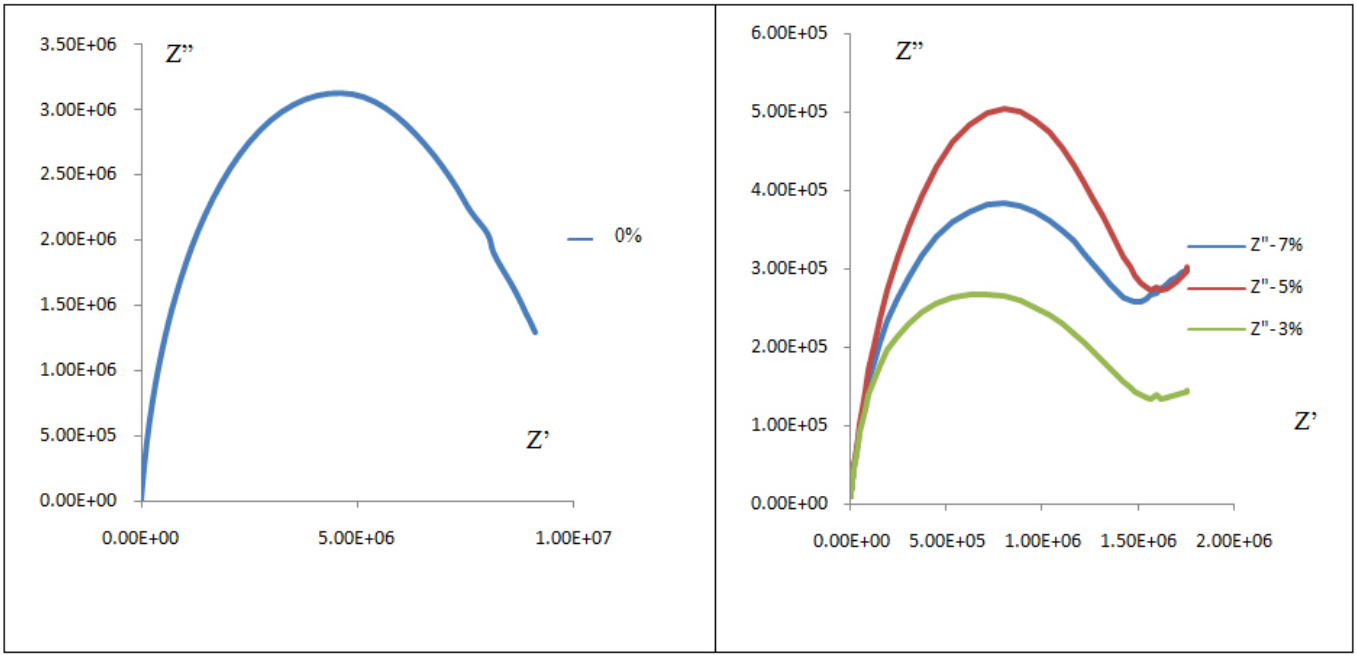

Figure 6 Nyquist plot, Z’ Vs Z” spectra for the samples 0 %, 3%, 5% and 7% AZO.

Table 3 Resistance, Capacitance and Conductivity values of the un-doped and AZO nanopowder.

Sample	Thickness (mm)	Resistance in MΩ	Capacitance x 10^{-11}F	Conductivity x 10^{-4}(Ω cm) $^{-1}$
ZnO (0%)	1.37	9.02	4.99	3.022
AZO (3%)	2.07	0.78	4.75	43.74
AZO (5%)	2.10	1.46	4.19	28.62
AZO (7%)	2.00	1.22	6.02	37.52

Impedance measurements. The impedance spectra of the real and imaginary parts of the impedance (i.e., Zs’ and Zs”, respectively) were obtained using Solartron SI1260 Impedance Gain-phase analyzer, in the frequency range, 1 to 100 MHz (1 V). All of the measurements were performed at room temperature for undoped ZnO and 3% , 5% and 7% AZO samples.

Fig (6) represents the relaxation times and resistance related to the bulk, grain boundaries and electrode interfaces in the complex impedance plane. The total impedance (semicircle arc) of the pure ZnO decreased significantly with Al doping. Then, the value seemed to increase with doping percentage and drops again for a doping of 7%. The Nyquist plot tended towards a second arc which is indicative of the doping influenced phase and may be due to the grain sizes and dipole dynamics [19,20]. Boukamp’s equivalent circuit software with non-linear least square (NLLS) fitting procedure is used to analyze the measured complex impedance data (Table 3). The impedance studies prove that electrical properties are significantly affected with variation in Al doping concentration to ZnO nanostructures.

IV. CONCLUSION

High crystalline un-doped and 0-7% Al-doped ZnO Nano powders were synthesized by simple microwave synthesis technique. From the TEM images of the as-synthesized powders, the mixture oxide precursors were mainly converted into nanocrystals with hexagonal structures, as shown in XRD data. In addition, the TEM-EDX images, SAED data, and the XRD pattern of the as-synthesized powders confirmed that Al^{3+} was incorporated into the ZnO lattices of wurtzite structure, and consequently the as-synthesized AZO Nano powders had a single phase of ZnO. The variation in the band gap of the samples could be attributed to defects introduced by the nature of the microwave synthesis, as well as dopant incorporation in other samples. A tenfold increase of conductivity, with Al doping, had been indicated in the Impedance Spectroscopy studies. In this study, the microwave technique for pure and Al doped ZnO synthesis is found to be a simpler, quicker and energy efficient method of synthesizing Nano powders. The structural, optical and electrical properties are significantly affected with variation in Al doping of the ZnO nanostructures.

V. REFERENCES

[1] V. A. Coleman and C. Jagadish , Zinc Oxide Bulk, Thin Films and Nanostructures, Elsevier Publishing, Australia, 2006.

[2] Mohammad Vaseem, Ahmad Umar and Yoon-Bong Hahn, Metal Oxide Nanostructures and Their Applications, American Scientific Publishers. 5(2010) 1–36.

[3] M. Ruba Devi, ZnO Nanoparticles structure and their influence on the growth rate of Cicer Arietinum, M. Phil. dissertation, University of Madras, Dec 2012.

[4] Selvakumari D, Deepa R, Mahalakshmi V, Subhashini P and Lakshminarayan N, Anti-Cancer Activity of ZnO Nanoparticles on MCF7 (Breast Cancer Cell) and A549 (Lung Cancer Cell) ARPN J. of Eng. and App. Sci, 10(12) (2015) 5418-5421.

[5] Xiao Wei Sun and Yi Yang, ZnO Nanostructures and their Applications, Pan Stanford Publishing, Singapore, 2012.

[6] Vinh Ai Dao, Tran Le, Tuan Tran, Huu Chi Nguyen, Kyunghae Kim, Jaehyeong Lee, Sungwook Jung, N. Lakshminarayan and Junsin Yi, Electrical and optical studies of transparent conducting ZnO:Al thin films by magnetron dc sputtering, J Electroceram., 23 (2-4), (2009)356-360.

[7] M. Mozibur Rahman, M. K. R. Khan, M. Rafiqul Islam, M. A. Halim, M. Shahjahan, M. A. Hakim, Dilip Kumar Saha and Jasim Uddin Khan, Effect of Al Doping on Structural, Electrical, Optical and Photoluminescence Properties of Nano-Structural ZnO Thin Films J. Mater. Sci. Technol. 28(4)(2012) 329-335.

[8] K. Kaviyarasu, Prem Anand Devarajan, A convenient route to synthesize hexagonal pillar shaped ZnO nano needles via CTAB surfactant, Adv. Mat. Lett., 4(7) (2013)582-585.

[9] Seungho Cho, Seung-Ho Jung, and Kun-Hong Lee, Morphology-Controlled Growth of ZnO Nanostructures Using Microwave Irradiation: from Basic to Complex Structures J. Phys. Chem. C, 112 (2008) 12769–12776.

[10] Zhiyong Fan and Jia G. Lu, Zinc Oxide Nanostructures: Synthesis and Properties, J of Nano. Sci. and Nano. Tech, 5(10), (2005) 1561-1573 (13).

[11] Faheem Ahmed, Shalendra Kumar, Nishat Arshi, M. S. Anwar, Ram Prakash, Growth and characterization of ZnO nanorods by microwave-assisted route: green chemistry approach, Adv. Mat. Lett., 2(3) (2011) 183-187.

[12] Amir Kajbafvala, Saeid Zanganeh, Ehsan Kajbafvala, H.R. Zargar, M. R. Bayati, S. K. Sadrnezhaad, Microwave-assisted synthesis of narcis-like zinc oxide nanostructures, J. of Alloys and Compounds 497 (2010) 325–329.

[13] Virendra Chandore, Gopal Carpenter, Ravindra Sen, Nitish Gupta, Synthesis of nano crystalline ZnO by Microwave Assisted Combustion method: An eco-friendly and solvent free route, Int J of Env. Sci: (IJESDM) 4(2)(2013) 45-47.

[14] F Zahedi, R S Dariani , S. M. Rozati, Structural, Optical and Electrical Properties of ZnO Thin Films Prepared by Spray Pyrolysis: Effect of Precursor Concentration, Bull Mater Sci 37: (2014)433-439.

[15] A. Khorsand Zak, R. Razali, W. H. Abd Majid and Majid Darroudi, Synthesis and characterization of a narrow size distribution of zinc oxide nanoparticles, Int. J. of Nanomedicine 6 (2011) 1399–1403.

[16] Vijay Kumar, M. Gohain, S. Som, Vinod Kumar, B. C. B. Bezuindenhoudt and Hendrik C. Swart, Microwave assisted synthesis of ZnO nanoparticles for lighting and dye Removal application, Physica B (2015), http://dx.doi.org/10.1016/j.physb.2015.07.020i

[17] M. C. Jun, S. U. Park and J. H. Koh, Comparative studies of Al-doped ZnO and Ga-doped ZnO transparent conducting oxide thin films, Nano Lett., 7, (2012)639.

[18] S. H. Park, S. E. Park, J. C. Lee, P. K. Song and J. H. Lee, Photoluminescence Characterization of Al-Doped ZnO Films Deposited by Using DC Magnetron Sputtering J. Korean Phy. Soc., 54, (2009)1344.

[19] M. Becerril, H. Silva-Lopez, A. Guillen-Cervantes, and O. Zelaya-Angel Aluminum-doped ZnO polycrystalline films prepared by co-sputtering of a ZnO-Al target, Revista Mexicana De F´Isica 60 (2014) 27–31.

[20] Xinghua Liang, Qingqing Song, Yusi Liu, Hao Liu, Preparation of ZnO Porous Nanostructures and Its Application in Cathode Material for Lithium Sulfur Battery, Int. J. Electrochem. Sci., 10 (2015) 9333 - 9341.